Neurochem Res (2014) 39:1797–1808
DOI 10.1007/s11064-014-1390-3

ORIGINAL PAPER

Linolenic Acid Provides Multi-cellular Protective Effects After Photothrombotic Cerebral Ischemia in Rats

Yang Liu · Qian Sun · Xiaojing Chen · Liang Jing · Wei Wang · Zhiyuan Yu · Guibing Zhang · Minjie Xie

Received: 14 March 2014 / Revised: 2 July 2014 / Accepted: 15 July 2014 / Published online: 26 July 2014

Abstract Alpha-linolenic acid (LIN) has been shown to provide neuroprotective effects against cerebral ischemia. LIN is a potent activator of TREK-1 channel and LIN-induced neuroprotection disappears in Trek1−/− mice, suggesting that this channel is directly related to the LIN-induced resistance of brain against ischemia. However, the cellular mechanism underlying LIN induced neuroprotective effects after ischemia remains unclear. In this study, using a rat photochemical brain ischemia model, we investigated the effects of LIN on the protein abundance of astrocytic glutamate transporter and AQP4, microglia activation, cell apoptosis and behavioral recovery following ischemia. Administration of LIN rescued the protein abundance of astrocytic glutamate transporter GLT-1, decreased the protein abundance of AQP4 and brain edema, inhibited microglia activation, attenuated cell apoptosis and improved behavioral function recovery. Meanwhile, TREK-1 was widely distributed in the cortex and hippocampus, primarily localized in astrocytes and neurons. LIN could potentiate the TREK-1 mediated astrocytic passive conductance and hyperpolarize the membrane potential. Our results suggest that LIN provides multiple cellular neuroprotective effects in cerebral ischemia. TREK-1 may serve as a promising multi-mechanism therapeutic target for the treatment of stroke.

Keywords TREK-1 · Cerebral ischemia · Neurovascular unit · Neuroprotection · Polyunsaturated fatty acids

Y. Liu · Q. Sun · X. Chen · L. Jing · W. Wang · Z. Yu · M. Xie (✉)
Department of Neurology, Tongji Hospital, Tongji Medical College, Huazhong University of Science and Technology, Wuhan 430030, People's Republic of China
e-mail: xie_minjie@126.com

W. Wang · M. Xie
Key Laboratory of Neurological Diseases (HUST), Ministry of Education of China, Wuhan 430030, Hubei, People's Republic of China

G. Zhang
Department of Neurology, Xiangyang Hospital Affiliated to Hubei University of Medicine, Xiangyang, People's Republic of China

Introduction

The neuroprotective effects of polyunsaturated fatty acids (PUFAs) and particularly alpha-linolenic acid (LIN) have been well established in numerous central nervous system (CNS) diseases [1–3]. Both in vitro and in vivo studies have shown LIN protects neurons against hyperexcitability-induced neuronal death and transient spinal cord ischemia [3–5]. PUFAs are potent protectors against focal and global ischemia [1, 3]. However, the cellular mechanisms underlying LIN induced neuroprotective effects are not fully clarified. The newly discovered TREK-1 channel (TWIK related K^+ channel) has been demonstrated to play a critical role in the LIN-induced resistance to brain ischemia since this neuroprotection disappears in Trek1−/− mice [6]. Meanwhile, LIN is known to potently activate the TREK-1 channel [7, 8].

TREK-1 is a member of newly discovered two-pore domain background potassium channels which contribute to the background leak K+ currents and play an important role in regulating neuronal excitability [7]. Several studies show a broad distribution of TREK-1 in neuronal, glial and vascular elements in the rat brain [1, 9–11]. TREK-1 activity is modulated by membrane stretch, intracellular acidification, temperature, volatile general anaesthetics and

polyunsaturated fatty acids (PUFAs), which qualifies as a signal integrator responsive to a wide range of physiological and pathological stimuli [12]. TREK-1 has been shown to play a key role in the cellular mechanisms of neuroprotection after cerebral ischemia [6, 13].

In the present study, we investigated the TREK-1 expression and cytoprotective effects of alpha-linolenic acid in a rat photochemical brain ischemia model. Our results show that administration of LIN restores the protein abundance of astrocytic glutamate transporter GLT-1, decreases the protein abundance of AQP4 and edema, and suppresses microglia activation, contributing to the reduction of cell apoptosis and behavioral function recovery of rats after focal ischemia.

Experimental Procedures

Animal Model Preparation

All the experiments were performed in accordance with the guidelines approved by the National Institute of Health Guide for the Care and Use of Laboratory Animals and the Institutional Animal Care and Use Committee at Tongji Medical College.

Adult male Sprague–Dawley rats weighing between 220 and 270 g were randomly assigned into control, sham-operated, ischemia, vehicle-treatment, and alpha-linolenic acid (LIN)-treatment groups. The experiments about the TREK-1 expression profile in central nervous system were carried out in normal rats. Photochemical ischemia was performed as previously described [14, 15]. In brief, the animals were anesthetized with enflurane mixed with 70 % N_2O/30 % O_2 gas delivered by a closely fit mask. Using aseptic technique, the scalp was incised and retracted to expose the scalp. Rose Bengal (7.5 mg/ml, dissolved in 0.9 % NaCl, Sigma Aldrich, USA) was given via a tail vein cannula at the dose of 0.133 ml/kg body weight. The rats were placed in a stereotaxic frame and irradiated by the cold light (15 W, 550 nm, KL1500LCD, Scott, Germany) at the region of 4 mm posterior to the bregma and 3.5 mm lateral from the midline for 20 min. Sham-operated rats were given saline instead. Body temperature was monitored with a rectal probe and maintained throughout the surgery at 37 ± 0.5 °C. Alpha-linolenic acid (Sigma Aldrich, USA) was administrated intra-cerebroventricularly (100 μM, 5 μL) at 30 min before photochemical ischemia. The dose used was selected based on our pilot studies on rats searching for the best protection (data not shown) and those reported previously [3]. Vehicle-treated animals received the same volumes of 0.9 % NaCl. Experimental rats were sacrificed on day 1, day 3, day 7, and day 14 respectively after focal ischemia.

Hippocampal Slice Preparation

Hippocampal slices were prepared from 3- to 4- week-old Sprague–Dawley (SD) rats. Animals were anesthetized with 100 % CO_2 before decapitation and their brains were removed from the skull and placed in an ice-cold, oxygenated (5 % CO_2/95 % O_2, pH = 7.4) slice preparation solution containing (in mM): 26 $NaHCO_3$, 1.25 NaH_2PO_4, 2.5 KCl, 10 $MgCl_2$, 10 glucose, 0.5 $CaCl_2$, 240 sucrose. Final osmolarity was 350 ± 2 mOsm. Coronal slices of 300 μm thickness were cut with a Vibratome (Pelco 1500) and transferred to a nylon slice holder basket immersed in artificial cerebral spinal fluid (aCSF) containing (in mM): 125 NaCl, 25 $NaHCO_3$, 10 glucose, 3.5 KCl, 1.25 NaH_2PO_4, 2.0 $CaCl_2$, 1 $MgCl_2$ (osmolarity 295 ± 5 mOsm) at room temperature (20–22 °C). The slices were kept in aCSF with continuous oxygenation for at least 60 min. before recording.

Electrophysiology

For in situ recording, individual hippocampal slices were transferred into the recording chamber which was constantly perfused with oxygenated aCSF (2.0 ml/min). Astrocytes located in the CA1 region were identified by infrared-differential interference contrast (IR-DIC) video microscopy (Olympus BX51W1) using a 40× water immersion objective and an IR-sensitive CCD camera with the images displayed on a monitor. Whole-cell membrane currents were amplified by a MultiClamp 700B amplifier, sampled by a DIGIDADA 1322A Interface, and the data acquisition was controlled by pClamp 9.0 software (all from Axon Instruments Inc., Foster City, CA, USA) installed on a Dell personal computer. The patch pipettes were fabricated from borosilicate capillaries (OD: 1.5 mm, Warner Instrument Corporation, Hamden, CT, USA) using a Flaming/Brown Micropipette Puller (Model P-97, Sutter Instrument Co., Novato, CA, USA). When filled with KCl-based pipette solution (140 KCl, 0.5 Ca_2Cl, 1.0 $MgCl_2$, 5 EGTA, 10 HEPES, 3 Mg-ATP, 0.3 Na-GTP (pH = 7.3, 290 ± 5 mOsm), the open pipette resistance was 3–5 MΩ. Membrane potential (Vm) was read in the "I = 0" mode when astrocytes were in voltage clamp recording mode, or directly measured in current clamp mode. The membrane capacitance (C_M), membrane resistance (R_M) and access resistances (R_a) were measured from the "Membrane test" protocol built into the pClamp 9.0. An average of R_a value of 15 MΩ was the most common and stable R_a value achieved routinely in mature astrocytes from rats older than 3 weeks. Also in all the pharmacological studies, the recordings having the Ra value varied greater than 10 % throughout experiment were excluded from the data analyses.

Nissl Staining, Immunohistochemical Staining and TUNEL Staining

Animals were given an overdose of anaesthetic and sacrificed by decapitation. The brain were removed and rapidly frozen in nitrogen-cooled isopentane, and stored in −80 °C until processing. The brain tissues were cut at 10 μm thickness at the level of −4.0 mm relative to bregma and mounted to poly-L-lysine coated slides. Nissl staining was performed to determine the neuronal cells loss and the general histologic features of the tissues in the cortex. The tissue sections were placed in 1 % toluidine blue for 5 min, and then rinsed under tapping water for 5 min, dehydrated in graded alcohols, cleared in xylene and mounted on slides. For immunohistochemical staining, the cryostat sections were fixed for 15 min by ice-cold 4 % paraformaldehyde in 0.1 M phosphate-buffered saline and then permeablized by 0.25 % Triton-X100 in PBS. The cryosections were treated with 10 % bovine serum albumin to bind non-specific antigen for 2 h at room temperature and then incubated with primary antibody at 4 °C overnight. The following primary antibodies were used: rabbit anti-TREK-1 (1:200, Alomone Labs, Israel), mouse anti-GFAP (1:200, Neomarkers, USA), rabbit-anti-Ki67 (1:100, Merck Millipore, USA), rabbit anti-Iba1 (1:200, Wako, Japan), and mouse anti-AQP4 (1:100, Santa Cruz, USA). As negative controls, the primary antibody for TREK-1 was blocked with immunizing peptides from the suppliers. For negative controls of other primary antibodies, we used nonspecific IgG instead of the primary antibody. After incubation of primary antibodies and rinsed with 0.01 M PBS, the sections were incubated with corresponding secondary antibodies (Cy3-conjugated anti-rabbit or FITC-conjugated anti-mouse IgG; 1:400, Cy3-conjugated anti-mouse, 1:400, FITC-conjugated anti-rabbit IgG; 1:400, Jackson ImmunoResearch Laboratories, USA) for 1 h at room temperature. The cryosections were rinsed three times with PBS and mounted in 50 % glycerol/0.01 % NaN_3 in PBS. Sections were observed blindly under Laser scanning confocal microscope (Olympus, FV500, Japan). Data were collected by sequential excitation to minimize "bleed through". All images were acquired under the same exposure time. The TREK-1 immunoreactivity was observed in five different fields in the boundary zone per section, three section per animal (n = 5). The number of Iba1 positive cells and DAPI in five different fields of boundary zone per section, three section per aninal (n = 5) was counted using a defined rectangular field area (×40 objective) with image soft (NIH Image, USA) by an observer blinded to the research.

To determine the percentage of cell death, terminal deoxynucleotidyl transferase–mediated deoxyuridine triphosphate nick-end labeling (TUNEL) staining was performed using the Red In situ Apoptosis Detection Kit (Merck Millipore, USA) strictly according to the manufacture's protocol. Then the slices were co-stained with DAPI (10 μg/ml, Sigma Aldrich, USA). The total number of TUNEL positive cells and DAPI in the five fields of the ischemic border area per section, three section per animal (n = 5) was counted with soft image (NIH Image, USA). The results were observed blindly under an Olympus BX-51 fluorescence microscope.

Western Blot

Animals were euthanized by deep anesthesia at observation times. The peri-infarct area is easily distinguished from the ischemia core due to the pale appearance of the infarct tissue. The peri-infarct cortex (2 mm × 2 mm × 2 mm) was quickly removed and was homogenized by sonification in RIPA lysis buffer with protease inhibitor cocktail (Roche, USA). After centrifugation of 12,000×*g* at 4 °C for 15 min, the supernatants were collected and the protein concentration was detected by a BCA Kit (Pierce, USA). Then the proteins were mixed with loading buffer (31.2 mM Tris, 1 % sodium dodecyl sulfate, 5 % glycerol, and 2.5 % β-mercaptoethanol) and boiled for 5 min. Samples containing 50 μg total protein were loaded on 12 % SDS-PAGE. After electrophoresis, the proteins were transferred to nitrocellucose membrane (0.45 μm, Millipore, USA). The non-specific binding was blocked by 5 % non-fat milk in TBS containing 0.1 % Tween-20 for 2 h at room temperature. The membranes were then incubated with the following primary antibody: rabbit anti-β-actin (1:1,000, Santa Cruz, USA), rabbit anti-TREK-1 (1:500, Alomone, Israel), rabbit anti-GLT-1 (1:500, Cell Signaling, USA), rabbit anti-GLAST (1:300, Santa Cruz, USA) and mouse anti-AQP4 (1:300, Santa Cruz, USA) overnight at 4 °C. Thereafter, the membranes were incubated with horseradish peroxidase conjugated IgG (1:5,000, Santa Cruz, USA) for 1 h at room temperature and visualized with ECL kit (Pierce, USA). The integrated optical density (OD) of signals was semi-quantified by Kodak Digital Science 1D system. The integrated optical density (OD) of the signals was semi-quantified and expressed as the ratio of OD from the tested proteins to OD from β-actin.

Measurement of Brain Water Content

Water content of the ischemic hemisphere was determined to evaluate the brain edema after focal ischemia. After division into right and left hemispheres along the midline, the ischemic hemispheres were immediately weighed precisely (wet weight). Then the tissues were dried for 24 h at 100 °C and weighed again (dry weight). The brain water

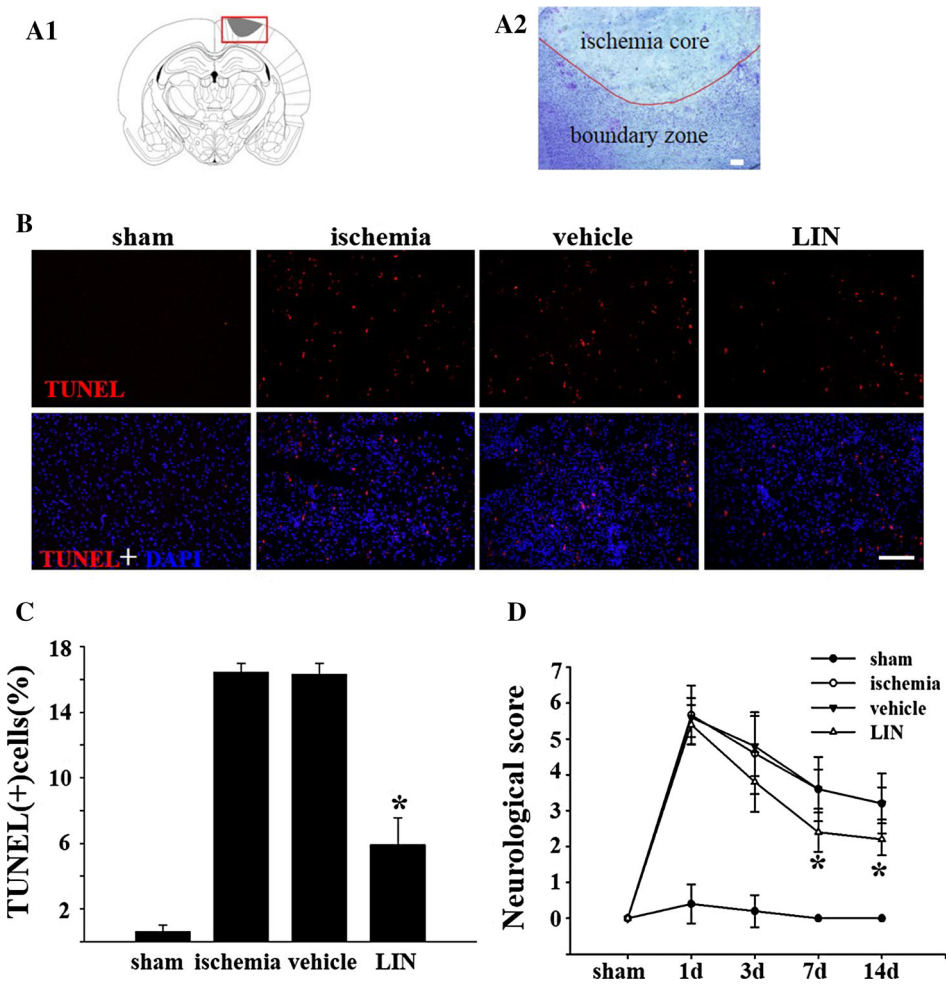

Fig. 1 Linolenic acid reduces cell apoptosis and contributes to functional recovery after focal ischemia **a**1 Schematic of photochemical ischemia model. The *dark area* shows the infarct core which is surrounded by the boundary zone (*red frame*) where we took images for analysis. **a**2 The nissl staining on day 7 post ischemia indicates an infarct lesion with neuronal cells loss. **b** Apoptotic cells in the cortex on day 3 after ischemia were detected by double staining of TUNEL (*red*) and DAPI (*blue*) in sham, ischemia, vehicle and LIN groups. *Scale bar* 100 μm. **c** Statistic analysis of percentage of TUNEL (+) cells at 3 days post-ischemia in sham, ischemia, vehicle and LIN treatment groups. **d** Statistic analysis of neurological deficit score evaluated before and after ischemia in sham, ischemia, vehicle and LIN treatment groups. Values are expressed as mean ± SD (n = 5). *$p < 0.05$ LIN treatment groups versus vehicle treatment groups by one-way ANOVA (Color figure online)

content was calculated by the formula: water content = 100 % (wet weight − dry weight)/wet weight.

Behavioral Measurements

All animals were operated on and tested in parallel. In all animals of the 2-week group, behavioral tests were performed before and on days 1, 3, 7, 14 after photochemically induced ischemia by a blinded investigator as previously described method [16]. A set of modified Neurological Severity Scores (NSS) composite of motor, sensory, and reflex tests were used to evaluate the functional impairment, including flexion of forelimb, flexion of hindlimb, head movement, floor walking, pinna reflex, corneal reflex, startle reflex and abnormal movements. Neurological function is graded on a scale 0 (normal score) to 10 (maximal deficit score).

Statistical Analysis

Statistical analyses were performed using SPSS 13.0. Statistically significant differences between data were evaluated by Student's *t* test or one-way analysis of variance (ANOVA) followed by turkey' post hoc test. Significance was considered at $p < 0.05$.

Results

Alpha-Linolenic Acid Inhibits Cell Apoptosis and Improves Behavioral Recovery After Focal Ischemia

In this study, we used the photochemical model to induce a consistently reproduced small cortical infarct (about 4 mm wide and 2 mm deep) in cerebral cortex (Fig. 1a1). After photochemical ischemia operation, rats had a higher survival rate in contrast to MCAO induced focal ischemia. Nissl staining revealed a dramatic neuronal loss in the cortex corresponding to ischemia core on day 7 following ischemia (Fig. 1a2). The adjacent cortex (about 1 mm wide around the margin of infarct) was depicted as boundary

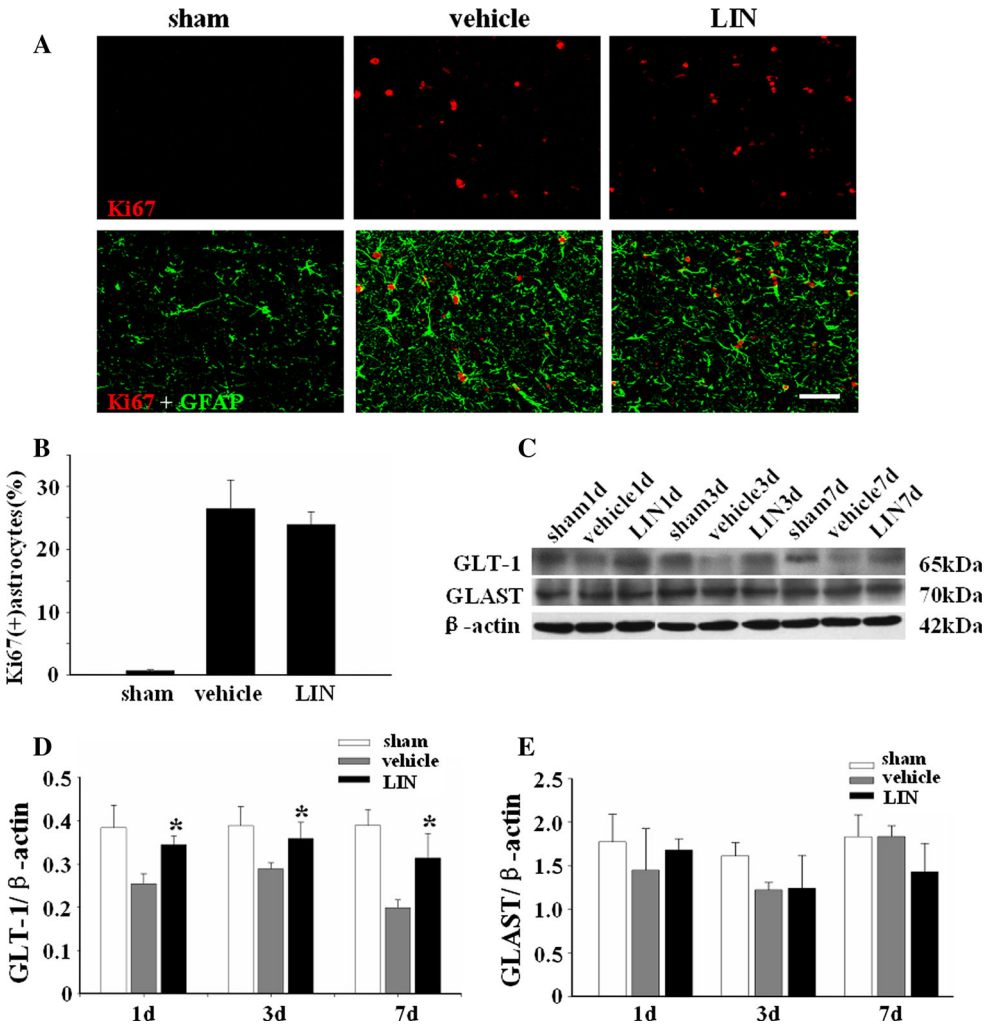

Fig. 2 Effect of linolenic acid on astrocytic proliferation and glutamate transporter protein abundance after ischemia. **a** Double immunofluorescent staining of GFAP (*green*) and Ki67 (*red*) in the boundary zone at day 3 post-ischemia. *Scale bar* 50 μm. **b** Quantitative analysis of percentage of Ki67 (+) astrocytes under sham, vehicle and LIN treatment groups. **c** Representative western blots of GLT-1, GLAST and β-actin expression in sham, vehicle and LIN treatment groups. **d** Statistic analysis of western blots signals of GLT-1 in sham, vehicle and LIN treatment groups on days 1, 3, 7 after ischemia. **e** Statistic analysis of western blots signals of GLAST in each group after ischemia. Values are expressed as mean ± SD (n = 5). $^{*}p < 0.05$ LIN treatment group versus vehicle group by one-way ANOVA (Color figure online)

zone where reactive gliosis could be detected (data not shown).

To assess the effect of LIN on cell apoptosis after focal ischemia, the double staining of TUNEL and DAPI was performed. As shown in Fig. 1b, TUNEL positive cells were rarely observed in the cortex of sham-operated groups. On day 3 after ischemia, the TUNEL positive cells increased significantly in the ischemic boundary zone of cortex in ischemia and vehicle groups whereas there was no significant difference between ischemia group and vehicle group. In rats receiving LIN, the percentage of TUNEL positive cells was reduced significantly compared to that of vehicle group (Fig. 1b, c).

We further studied the effect of LIN on neurological outcome of rats after ischemia. All rats exhibited obvious function deficiency after ischemia. The neurological deficit scores of the ischemia and vehicle-treated groups were comparable which increased on day 1 after ischemia, and partially recovered spontaneously on days 3, 7 and 14. This indicates that the solvent in vehicle group induces marginal effects on both neuronal damage and functional recovery after focal ischemia. Administration of LIN significantly promoted the behavioral recovery on days 7, 14 compared with the vehicle-treated groups (Fig. 1d).

Effect of Alpha-Linolenic Acid on the Protein Abundance of Astrocytic GLT-1 After Focal Ischemia

Astrocytes play a fundamental role in the pathogenesis of ischemic neuronal death [17, 18]. Here we investigated the effect of LIN on astrocyte proliferation after ischemia. As shown in Fig. 2a, few Ki67 positive cells were observed in the cortex of sham control brain. On day 3 after ischemia, Ki67 positive cells increased significantly, indicating that cell proliferation occurred after ischemia. Double immunofluorescence of GFAP and Ki67 demonstrated that Ki67 positive cells co-localized well with GFAP positive astrocytes. However, the number of Ki67 positive astrocytes in the cortex of rats after LIN treatments showed no

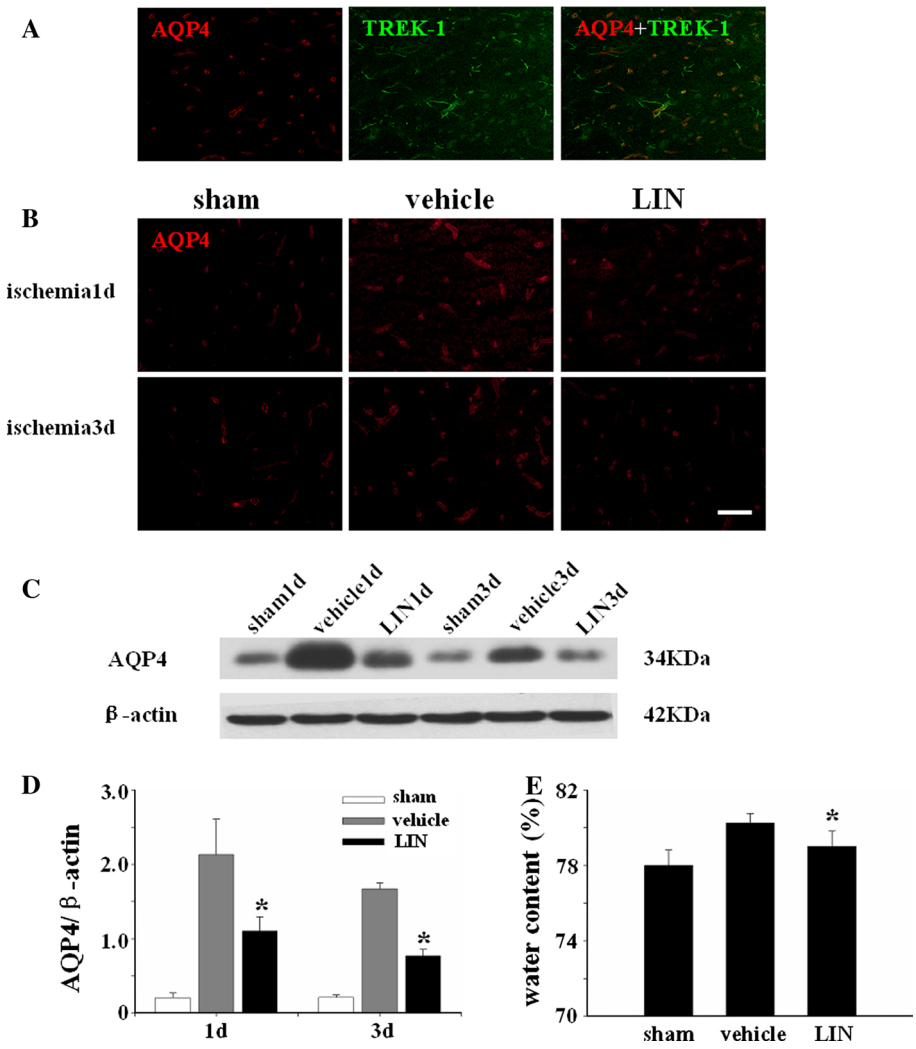

Fig. 3 Effect of linolenic acid on the protein abundance of AQP4 and brain water content. **a** Representative images of immunofluorescent staining of AQP4 (*red*) and TREK-1(*green*) in the cortex of sham rats. *Scale bar* 50 μm. **b** Immunofluorescent staining of AQP4 (*red*) in the boundary zone on day 3 post-ischemia of sham, vehicle and LIN treated rats. *Scale bar* 50 μm. **c** Representative western blots of AQP4 and β-actin expression in the boundary zone after ischemia. **d** Statistic analysis of western blots signals of AQP4 in the boundary zone of sham and vehicle, LIN treatment groups after ischemia. **e** Statistic analysis of brain water content of sham, vehicle, and LIN treatment groups. Values are expressed as mean ± SD (n = 5). *$p < 0.05$ LIN treatment groups versus vehicle treatment groups by one-way ANOVA (Color figure online)

significant change compared with that in vehicle ischemic group (Fig. 2a, b).

Astroglial glutamate transporters, GLT-1 and GLAST, play an essential role in removing released glutamate from the extracellular space to prevent glutamate-induced excitotoxicity [19]. The protein abundance of glutamate transporters extracted from the ischemic boundary zone was evaluated by western blot analysis. As shown in Fig. 2c–e, both the protein abundance of GLT-1 and GLAST were reduced after ischemia whereas GLT-1 presented much greater decrease than GLAST. After pretreatment with LIN intra-cerebroventricularly 30 min before ischemia, the protein abundance of GLT-1 was significantly rescued compared to vehicle groups (relative O.D., 0.344 ± 0.021 vs. 0.254 ± 0.023 on day 1, 0.359 ± 0.037 vs. 0.289 ± 0.014 on day 3, 0.313 ± 0.057 vs. 0.199 ± 0.019 on day 7 post ischemia, $p < 0.05$). Nevertheless, another subtype of astrocytic glutamate transporter GLAST showed no significant change after administration of LIN ($p > 0.05$) (Fig. 2c, e).

Alpha-Linolenic Acid Decreases the Protein Abundance of Aquaporin 4 and Reduces Edema After Focal Ischemia

AQP4 has been found to play a role in the pathophysiology of brain edema after ischemia [20]. In this study, we investigated the effect of LIN on the protein abundance of AQP4 and brain water content after ischemia. As shown in Fig. 3a, AQP4 immunostaining was co-localized with TREK-1, especially in the astrocyte endfeet covering blood vessels, in the cortex of sham-operated rats. After ischemia, the AQP4 immunoreactivity increased significantly in the boundary zone on day 1 and day 3 compared to sham-operated groups. However, after treatment with LIN, the immunoreactivity of AQP4 was reduced compared with that of vehicle groups (Fig. 3b). In agreement with the immunostaining results, the western blot analysis revealed that administration of LIN significantly reduced the protein abundance of AQP4 after focal ischemia compared with vehicle groups (1.102 ± 0.194 vs. 2.13 ± 0.475 on day 1,

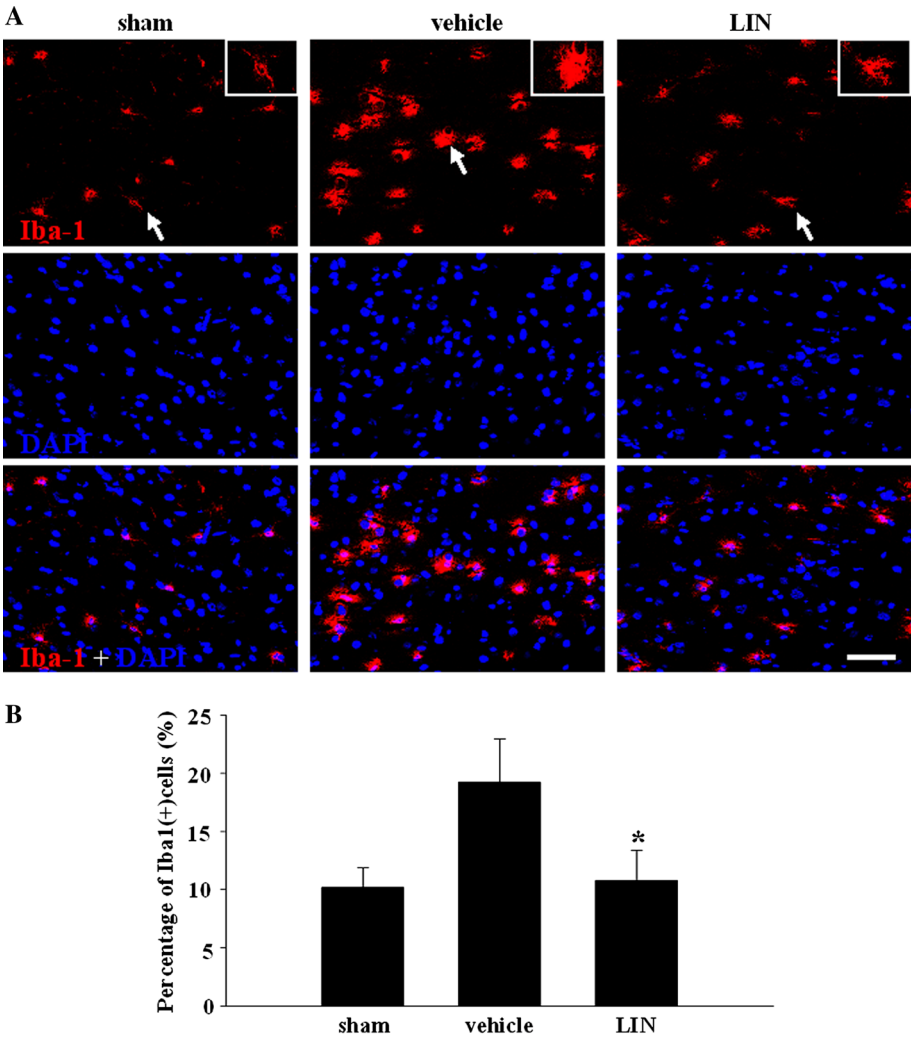

Fig. 4 Effect of linolenic acid on microglial activation **a** Representative images of double staining of Iba1 (*red*) and DAPI (*blue*) in the boundary zone at 24 h post-ischemia. *Scale bar* 50 μm. **b** Quantitative analysis of percentage of Iba1 (+) cells in sham, vehicle and LIN treatment groups. Values are expressed as mean ± SD (n = 5). *$p < 0.05$ LIN treatment groups versus vehicle groups by one-way ANOVA (Color figure online)

0.771 ± 0.087 vs. 1.67 ± 0.081 on day 3, $p < 0.05$) (Fig. 3c, d). Next, we studied the effect of LIN on brain edema development on day 1 after ischemia. Increased water content in the ipsilateral hemispheres was observed on day 1 post ischemia compared to sham-operated groups (0.803 ± 0.003 vs. 0.778 ± 0.003, $p < 0.05$); However, this edema was significantly attenuated by LIN treatment (0.793 ± 0.003 vs. 0.803 ± 0.003, $p < 0.05$) (Fig. 3e).

Effect of Alpha-Linolenic Acid on Microglia Activation After Focal Ischemia

Microglial activation is an early response to brain ischemia and microglial activation mediated inflammatory responses may exacerbate acute ischemic injury [21, 22]. We next investigated the effect of LIN on microglia activation after focal ischemia. Immunofluorescence revealed that the Iba1 positive microglia became activated characterized by the amoeboid morphology with an enlarged cell body and shortened processes in the boundary zone on day 1 after ischemia, while in the sham-operated groups, the microglia in resting state were mainly ramified (Fig. 4a). Moreover, the number of Iba1 positive microglia increased significantly compared with that in sham groups (Fig. 4a, b). However, administration with LIN significantly decreased the number of Iba1 positive microglia compared with vehicle groups (10.8 ± 1.5 % vs. 19.2 ± 2.1 %, $p < 0.05$). In addition, the cell body of microglia in LIN treatment groups was much smaller than that of the vehicle groups (Fig. 4a, b).

Expression of TREK-1 in the Cortex and Hippocampus

Previous study has shown that LIN-induced neuroprotection against ischemia is mediated by TREK-1 channel [6]. Here we studied the expression of TREK-1 in the cortex and hippocampus, areas susceptible to ischemic damage. Under normal condition, the TREK-1 immunoreactivity was widely observed in cortex, CA1 region and DG region of the hippocampus (Fig. 5a). According to the cellular morphological features of TREK-1-immunostained cells, both glia and neurons were labeled. Double immunofluorescent

analysis revealed that the TREK-1 immunoreactivity co-localized well with GFAP positive astrocytes in cortex (Fig. 5b).

Up-Regulated TREK-1 Expression in Reactive Astrocytes in Ischemic Boundary Zone After Focal Ischemia

Subsequently we investigated the temporal changes of TREK-1 protein expression after ischemia. Immunofluorescence staining demonstrated that the expression of TREK-1 was relatively low in sham operated animals. After ischemia, the TREK-1 immunoreactivity increased on day 3, peaked on day 7 whereas it decreased slightly on day 14 after ischemia. In addition, the up-regulation of TREK-1 was found to be paralleled with the enhanced expression of GFAP and swelling processes of astrocytes (Fig. 6a). To confirm our immunofluorescent findings, we assessed the changes of protein abundance of TREK-1 following focal ischemia by western blot analysis. Consistent with the immunofluorescence staining result, the TREK-1 immunoreactivity was elevated on day 3 and peaked on day 7 whereas decreased on day 14 after ischemia (Fig. 6b, c). Meanwhile, LIN treatment did not induce significant changes of TREK-1 protein abundance in the cortex of rats following ischemia compared with those in vehicle ischemic group (data not shown).

Effect of Alpha-Linolenic Acid on TREK-1 Mediated Astrocyte Passive Conductance

Our previous study has demonstrated that TREK-1 contributes significantly to the astrocytic characteristic passive conductance and helps to establish the highly negative membrane potential [23]. We now studied the effect of LIN on the conductance and membrane potential of astrocytes in hippocampal slice. As shown in Fig. 7a, changing the bath solutions from normal aCSF to aCSF containing LIN (10 μM) potentiated the passive conductance expressed in astrocytes. The mean current–voltage relationship from 4 recordings showed that 10 μM LIN increased 10 % of passive conductance at the command voltages of +20 and −160 mV (Fig. 7b). We next investigated the effect of LIN on the membrane potential of mature astrocytes in hippocampal slices. As shown in Fig. 7c, d, LIN could hyperpolarize membrane potential of astrocytes reversibly (from -89.30 ± 0.55 to -90.98 ± 0.46 mV, $n = 5$, $p < 0.05$).

Discussion

Recent research suggests that brain function and dysfunction are manifested at the level of cell–cell signaling between neuronal, glial and vascular (neurovascular unit) elements [24]. It is increasingly evident that therapeutic approaches that target these various players in the ischemic cascade hold considerable promise for the treatment of acute ischemic stroke [25]. Polyunsaturated fatty acids (PUFAs) and particularly LIN have been shown to provide neuroprotective effects against focal and global ischemia [1, 3]. The present study shows major cytoprotective effects upon several components of the neurovascular unit by LIN in rats following focal ischemia.

The neuroprotection induced by PUFAs against ischemia is related to their action on the TREK-1 channel since this neuroprotection disappears in Trek1−/− mice [6]. TREK-1 is widely distributed throughout the brain and spinal cord [6, 9, 10], whereas its cellular location remains

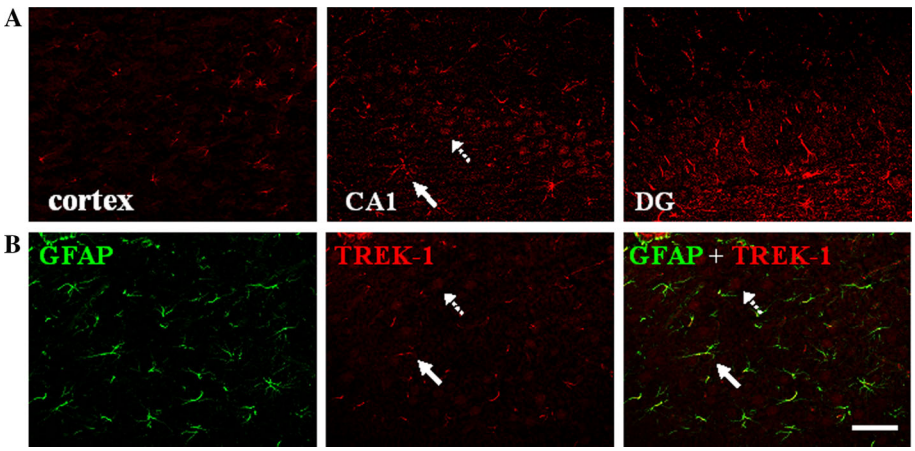

Fig. 5 Cellular localization of TREK-1 in cortex and hippocampus of rat brain. **a** Representative images of immunofluorescence of TREK-1 (*red*) in the region of cortex, CA1, dentate gyrus of hippocampus respectively. **b** Double immunofluorescence of TREK-1 (*red*) and GFAP (*green*) in cortex. *Solid arrow* indicates cell with astrocytic morphology. *Dashed arrow* indicates cells with neuronal morphology. *Scale bar* represents 50 μm (Color figure online)

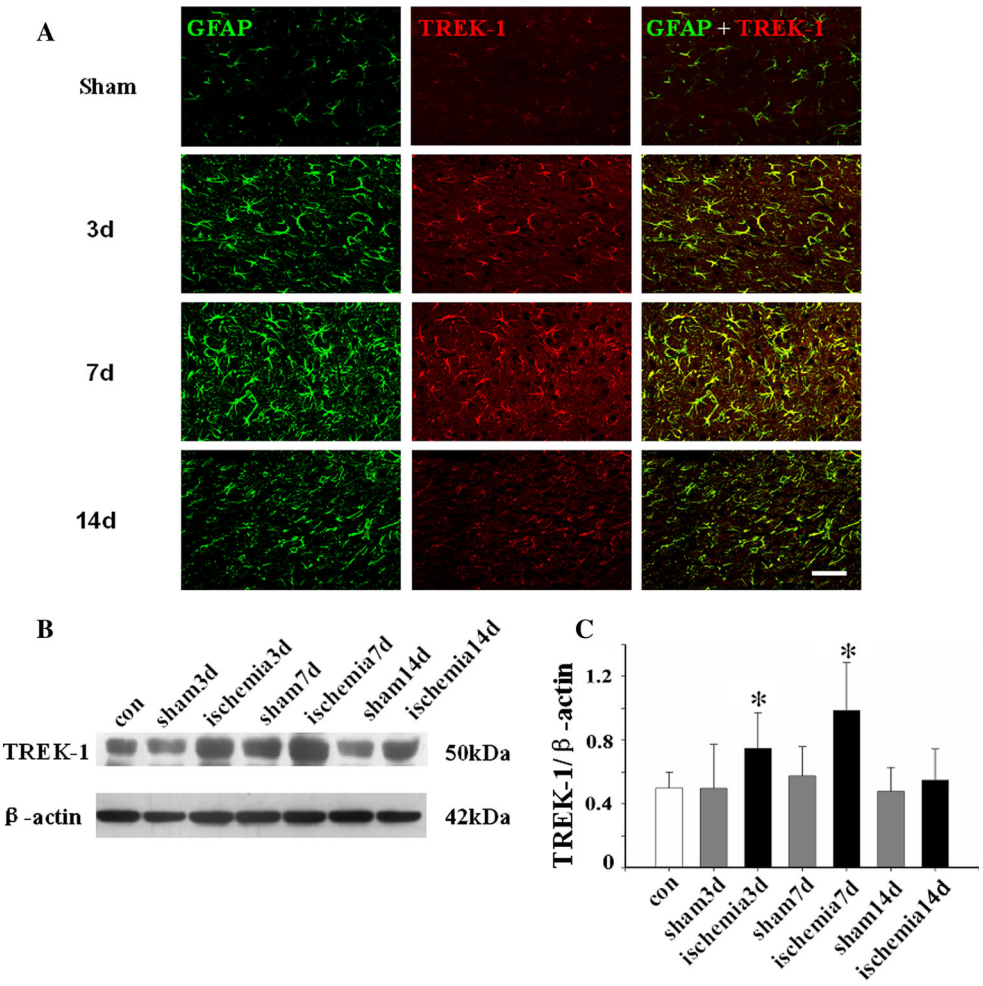

Fig. 6 Temporal changes of TREK-1 expression in the cortex after focal cerebral ischemia. **a** Double immunofluorescence of TREK-1 (*red*) and GFAP (*green*) in the boundary zone of rats in control and on day 3, day 7 and day 14 after focal cerebral ischemia. *Scale bar* represents 50 μm. **b** Representative western blots of TREK-1 and β-actin expression in the boundary zone after ischemia. **c** Statistic analysis of western blots signals of TREK-1 in the boundary zone of control, sham and ischemic rats. Values are expressed as mean ± SD (n = 5). $*p < 0.05$ ischemia groups versus sham groups by one-way ANOVA (Color figure online)

controversial. Early studies showed TREK-1 was found in cells with the morphology of neurons but not in cells with glial characteristics [9, 10]. However, recent data demonstrated the TREK-1 expression in astrocytes both in vivo and in vitro [23, 26, 27]. TREK-1 channel expression has also been found in the rat basilar artery and endothelial cells [2, 11]. In agreement with these results, we show that TREK-1 immunoreactivity displays a widespread distribution in the glial and neuronal cells in prefrontal cortex, CA1 region and DG region of the hippocampus (Fig. 5).

The established astrocytic homeostatic functions including glutamate uptake and K^+ buffering are exerted by a number of electrogenic transporters and exchangers, which are driven by the hyperpolarized membrane potential [28]. We previously have shown that TREK-1 contributes significantly to the astrocyte passive conductance and helps to set the hyperpolarized membrane potential [23]. Here we found that LIN could potentiate the astrocytic passive conductance and hyperpolarize the membrane potential (Fig. 7). Since TREK-1 channel is resistant to hypoxia and is activated with acidosis and arachidonic acid and other PUFAs [12, 29], conditions that accompany cerebral ischemia, the activation of TREK-1 might participate in repolarizing astrocytes to maintain the homeostatic function under ischemic conditions.

Glutamate excitotoxicity is one major mechanism underlying ischemic damage in the CNS [19]. It was hypothesized that impaired function of glial glutamate transporters induced by ischemia may lead to an elevated level of extracellular glutamate and subsequent excitotoxic neuronal death [30]. Potassium channels especially Kir4.1 and astrocytic glutamate transporter GLT-1 have been found to cooperate functionally whereby the activity of potassium channels assures a sufficient electrochemical potential to drive glutamate uptake via GLT-1 [31, 32]. We have previously shown that inhibition of TREK-1 activity with quinine suppressed the uptake of glutamate by astrocytes under hypoxia conditions [33]. Polyunsaturated fatty acids may also directly affect astrocytic glutamate transporters via the lipid environment [34]. As shown in this study, LIN could hyperpolarize the astrocyte resting membrane potential and rescue the decreased protein

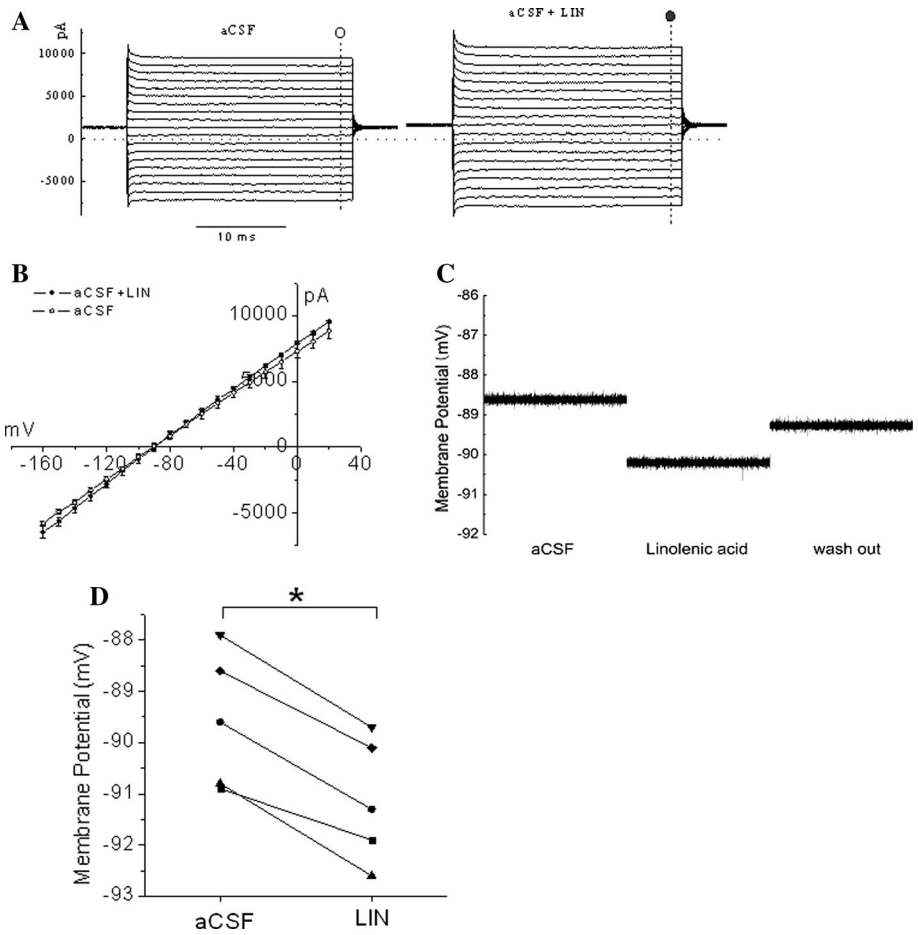

Fig. 7 Linolenic acid potentiates astrocyte passive conductance and hyperpolarizes membrane potential by whole-cell patch clamp recording. **a** Representative astrocyte whole-cell passive currents recorded first in aCSF and then after addition of linolenic acid (10 μM). For whole-cell recordings, the cells were held at −70 mV and the membrane currents were activated by stepping the recorded cell from −160 to +20 mV in 10 mV increments. The step duration was 50 ms and the consecutive steps were separated by a 1-s interval at −70 mV. **b** The mean current–voltage relationship shows that 10 μM linolenic acid potentates 10 % of passive conductance at the command voltages of −20 mV and +160 mV. **c** Representative membrane potential recordings in current clamp mode. The recordings show the membrane potential changes when the recorded astrocytes were exposed to aCSF and aCSF containing 10 μM linolenic acid. Each response was a 5 s segment taken at the steady-state level from a continuous recording. **d** Analysis of the effect of 10 μM linolenic acid on membrane potential of astrocytes. (n = 5, paired *t* test,* represents $p < 0.01$)

abundance of GLT-1 in the penumbra after focal ischemia (Figs. 2, 7).

Brain edema is a severe complication of stroke and is a major cause of disability and mortality in many neurological disorders. AQP4, the principle astrocytic water channel, has been shown to play a critical role in modulating the brain water transport and be involved in the formation and dissolution of brain edema [20]. Previous work demonstrated that AQP4 co-localized well with inwardly rectifying potassium channel Kir4.1, suggesting a functional coupling between these proteins [35–37]. In this study, we demonstrated AQP4 immunostaining was co-localized with TREK-1 and LIN down-regulated the expression of AQP4 in the penumbra and reduced brain tissue edema after cerebral ischemia (Fig. 3). The underlying mechanisms of the coupling between TREK-1 and AQP4 remain to be determined in the future study.

Cerebral ischemia results in intracellular acidosis, cell swelling and arachidonic acid release. These pathological mediators might contribute to the opening of TREK-1, which may hyperpolarize both presynaptic neurons and postsynaptic neurons and thus protect against glutamate excitotoxicity [38]. Meanwhile, the selective expression and activation of TREK-1 in brain collaterals has been shown to play a significant role in the protective mechanisms of polyunsaturated fatty acids against stroke by providing residual circulation during ischemia [2]. We have previously shown that inhibition of TREK-1 activity increased neuronal apoptosis in neuron and astrocyte coculture exposed to hypoxia [33]. Here we demonstrated

that LIN significantly reduced cell apoptosis and ameliorated neurological deficit after focal ischemia (Fig. 1). The neuronal protective effects of LIN may be mediated by multiple mechanisms including enhanced glutamate uptake capacity by astrocytes, reduction of AQP4 expression and brain edema, inhibition of microglia activation and increased neuronal resistance to glutamate excitotoxicity.

It should be noted that LIN may have multiple effects on glutamate receptors and ion channels besides TREK-1. It can partially inhibit voltage-sensitive Na^+ channels and voltage-sensitive Ca^{2+} channels [39–41]. LIN is a potent agonist of G-protein coupled free fatty acid (FFA) receptors that are widely distributed within the CNS [42, 43] and may potentially activate TREK-1 indirectly. Moreover, LIN can activate other background TREK-2 and TRAAK potassium channels [44–46]. Nevertheless, the polyunsaturated fatty acids including LIN induced neuroprotection is absent in Trek1−/− mice, indicating that protection by polyunsaturated fatty acids is primarily mediated by TREK-1 opening [6].

In summary, LIN provides multiple cellular neuroprotective effects in cerebral ischemia. The present data suggest that activation of TREK-1 provides a crucial multiple cellular neuroprotective mechanism in the ischemic pathology and might be a potential promising therapeutic target for stroke.

Acknowledgments The investigation was supported by the National Natural Science Foundation of China (30971007, 81371312, 81030021), Natural Science Foundation for outstanding young scholar of Hubei Province (2010CDA103) and National Basic Research Development Program (973 Program) of China (2011CB504403).

References

1. Heurteaux C, Laigle C, Blondeau N, Jarretou G, Lazdunski M (2006) Alpha-linolenic acid and riluzole treatment confer cerebral protection and improve survival after focal brain ischemia. Neuroscience 137:241–251
2. Blondeau N, Petrault O, Manta S, Giordanengo V, Gounon P, Bordet R, Lazdunski M, Heurteaux C (2007) Polyunsaturated fatty acids are cerebral vasodilators via the TREK-1 potassium channel. Circ Res 101:176–184
3. Lauritzen I, Blondeau N, Heurteaux C, Widmann C, Romey G, Lazdunski M (2000) Polyunsaturated fatty acids are potent neuroprotectors. EMBO J 19:1784–1793
4. Blondeau N, Widmann C, Lazdunski M, Heurteaux C (2001) Polyunsaturated fatty acids induce ischemic and epileptic tolerance. Neuroscience 109:231–241
5. Lang-Lazdunski L, Blondeau N, Jarretou G, Lazdunski M, Heurteaux C (2003) Linolenic acid prevents neuronal cell death and paraplegia after transient spinal cord ischemia in rats. J Vasc Surg 38:564–575
6. Heurteaux C, Guy N, Laigle C, Blondeau N, Duprat F, Mazzuca M, Lang-Lazdunski L, Widmann C, Zanzouri M, Romey G, Lazdunski M (2004) TREK-1, a K+ channel involved in neuroprotection and general anesthesia. EMBO J 23:2684–2695
7. Kim D (2005) Physiology and pharmacology of two-pore domain potassium channels. Curr Pharm Des 11:2717–2736
8. Fink M, Lesage F, Duprat F, Heurteaux C, Reyes R, Fosset M, Lazdunski M (1998) A neuronal two P domain K+ channel stimulated by arachidonic acid and polyunsaturated fatty acids. EMBO J 17:3297–3308
9. Hervieu GJ, Cluderay JE, Gray CW, Green PJ, Ranson JL, Randall AD, Meadows HJ (2001) Distribution and expression of TREK-1, a two-pore-domain potassium channel, in the adult rat CNS. Neuroscience 103:899–919
10. Talley EM, Solorzano G, Lei Q, Kim D, Bayliss DA (2001) Cns distribution of members of the two-pore-domain (KCNK) potassium channel family. J Neurosci 21:7491–7505
11. Bittner S, Ruck T, Schuhmann MK, Herrmann AM, Moha ou Maati H, Bobak N, Gobel K, Langhauser F, Stegner D, Ehling P, Borsotto M, Pape HC, Nieswandt B, Kleinschnitz C, Heurteaux C, Galla HJ, Budde T, Wiendl H, Meuth SG (2013) Endothelial TWIK-related potassium channel-1 (TREK1) regulates immune-cell trafficking into the CNS. Nat Med 19:1161–1165
12. Honore E (2007) The neuronal background K2P channels: focus on TREK1. Nat Rev Neurosci 8:251–261
13. Blondeau N, Lauritzen I, Widmann C, Lazdunski M, Heurteaux C (2002) A potent protective role of lysophospholipids against global cerebral ischemia and glutamate excitotoxicity in neuronal cultures. J Cereb Blood Flow Metab 22:821–834
14. Qu WS, Wang YH, Ma JF, Tian DS, Zhang Q, Pan DJ, Yu ZY, Xie MJ, Wang JP, Wang W (2011) Galectin-1 attenuates astrogliosis-associated injuries and improves recovery of rats following focal cerebral ischemia. J Neurochem 116:217–226
15. Watson BD, Dietrich WD, Busto R, Wachtel MS, Ginsberg MD (1985) Induction of reproducible brain infarction by photochemically initiated thrombosis. Ann Neurol 17:497–504
16. Schabitz WR, Berger C, Kollmar R, Seitz M, Tanay E, Kiessling M, Schwab S, Sommer C (2004) Effect of brain-derived neurotrophic factor treatment and forced arm use on functional motor recovery after small cortical ischemia. Stroke 35:992–997
17. Swanson RA, Ying W, Kauppinen TM (2004) Astrocyte influences on ischemic neuronal death. Curr Mol Med 4:193–205
18. Takano T, Oberheim N, Cotrina ML, Nedergaard M (2009) Astrocytes and ischemic injury. Stroke 40:S8–S12
19. Tanaka K, Watase K, Manabe T, Yamada K, Watanabe M, Takahashi K, Iwama H, Nishikawa T, Ichihara N, Kikuchi T, Okuyama S, Kawashima N, Hori S, Takimoto M, Wada K (1997) Epilepsy and exacerbation of brain injury in mice lacking the glutamate transporter GLT-1. Science 276:1699–1702
20. Manley GT, Fujimura M, Ma T, Noshita N, Filiz F, Bollen AW, Chan P, Verkman AS (2000) Aquaporin-4 deletion in mice reduces brain edema after acute water intoxication and ischemic stroke. Nature Med 6:159–163
21. Amantea D, Nappi G, Bernardi G, Bagetta G, Corasaniti MT (2009) Post-ischemic brain damage: pathophysiology and role of inflammatory mediators. FEBS J 276:13–26
22. Yenari MA, Kauppinen TM, Swanson RA (2010) Microglial activation in stroke: therapeutic targets. Neurotherapeutics 7:378–391
23. Zhou M, Xu G, Xie M, Zhang X, Schools GP, Ma L, Kimelberg HK, Chen H (2009) TWIK-1 and TREK-1 are potassium channels contributing significantly to astrocyte passive conductance in rat hippocampal slices. J Neurosci 29:8551–8564
24. Guo S, Lo EH (2009) Dysfunctional cell–cell signaling in the neurovascular unit as a paradigm for central nervous system disease. Stroke 40:S4–S7
25. Zhang L, Zhang ZG, Chopp M (2012) The neurovascular unit and combination treatment strategies for stroke. Trends Pharmacol Sci 33:415–422

26. Chu KC, Chiu CD, Hsu TT, Hsieh YM, Huang YY, Lien CC (2010) Functional identification of an outwardly rectifying pH- and anesthetic-sensitive leak K(+) conductance in hippocampal astrocytes. Eur J Neurosci 32:725–735
27. Woo DH, Han KS, Shim JW, Yoon BE, Kim E, Bae JY, Oh SJ, Hwang EM, Marmorstein AD, Bae YC, Park JY, Lee CJ (2012) TREK-1 and Best1 channels mediate fast and slow glutamate release in astrocytes upon GPCR activation. Cell 151:25–40
28. Olsen ML, Sontheimer H (2008) Functional implications for Kir4.1 channels in glial biology: from K+ buffering to cell differentiation. J Neuroche 107:589–601
29. Buckler KJ, Honore E (2005) The lipid-activated two-pore domain K+ channel TREK-1 is resistant to hypoxia: implication for ischaemic neuroprotection. J Physiol 562:213–222
30. Ouyang YB, Voloboueva LA, Xu LJ, Giffard RG (2007) Selective dysfunction of hippocampal CA1 astrocytes contributes to delayed neuronal damage after transient forebrain ischemia. J Neurosci 27:4253–4260
31. Olsen ML, Campbell SC, McFerrin MB, Floyd CL, Sontheimer H (2010) Spinal cord injury causes a wide-spread, persistent loss of Kir4.1 and glutamate transporter 1: benefit of 17 beta-oestradiol treatment. Brain 133:1013–1025
32. Kucheryavykh YV, Kucheryavykh LY, Nichols CG, Maldonado HM, Baksi K, Reichenbach A, Skatchkov SN, Eaton MJ (2007) Downregulation of Kir4.1 inward rectifying potassium channel subunits by RNAi impairs potassium transfer and glutamate uptake by cultured cortical astrocytes. Glia 55:274–281
33. Wu X, Liu Y, Chen X, Sun Q, Tang R, Wang W, Yu Z, Xie M (2013) Involvement of TREK-1 activity in astrocyte function and neuroprotection under simulated ischemia conditions. J Mol Neurosci 49:499–506
34. Volterra A, Trotti D, Cassutti P, Tromba C, Galimberti R, Lecchi P, Racagni G (1992) A role for the arachidonic acid cascade in fast synaptic modulation: ion channels and transmitter uptake systems as target proteins. Adv Exp Med Biol 318:147–158
35. Nagelhus EA, Mathiisen TM, Ottersen OP (2004) Aquaporin-4 in the central nervous system: cellular and subcellular distribution and coexpression with Kir4.1. Neuroscience 129:905–913
36. Nagelhus EA, Horio Y, Inanobe A, Fujita A, Haug FM, Nielsen S, Kurachi Y, Ottersen OP (1999) Immunogold evidence suggests that coupling of K+ siphoning and water transport in rat retinal Muller cells is mediated by a coenrichment of Kir4.1 and AQP4 in specific membrane domains. Glia 26:47–54
37. Strohschein S, Huttmann K, Gabriel S, Binder DK, Heinemann U, Steinhauser C (2011) Impact of aquaporin-4 channels on K+ buffering and gap junction coupling in the hippocampus. Glia 59:973–980
38. Franks NP, Honore E (2004) The TREK K2P channels and their role in general anaesthesia and neuroprotection. Trends Pharmaco Sci 25:601–608
39. Benoit E, Escande D (1991) Riluzole specifically blocks inactivated Na channels in myelinated nerve fibre. Pflugers Arch 419:603–609
40. Hebert T, Drapeau P, Pradier L, Dunn RJ (1994) Block of the rat brain IIA sodium channel alpha subunit by the neuroprotective drug riluzole. Mol Pharmacol 45:1055–1060
41. Huang CS, Song JH, Nagata K, Yeh JZ, Narahashi T (1997) Effects of the neuroprotective agent riluzole on the high voltage-activated calcium channels of rat dorsal root ganglion neurons. J Pharmacol Exp Ther 282:1280–1290
42. Briscoe CP, Tadayyon M, Andrews JL, Benson WG, Chambers JK, Eilert MM, Ellis C, Elshourbagy NA, Goetz AS, Minnick DT, Murdock PR, Sauls HR Jr, Shabon U, Spinage LD, Strum JC, Szekeres PG, Tan KB, Way JM, Ignar DM, Wilson S, Muir AI (2003) The orphan G protein-coupled receptor GPR40 is activated by medium and long chain fatty acids. J Biol Chem 278:11303–11311
43. Ma D, Tao B, Warashina S, Kotani S, Lu L, Kaplamadzhiev DB, Mori Y, Tonchev AB, Yamashima T (2007) Expression of free fatty acid receptor GPR40 in the central nervous system of adult monkeys. Neurosci Res 58:394–401
44. Duprat F, Lesage F, Patel AJ, Fink M, Romey G, Lazdunski M (2000) The neuroprotective agent riluzole activates the two P domain K(+) channels TREK-1 and TRAAK. Mol Pharmacol 57:906–912
45. Lesage F, Lazdunski M (2000) Molecular and functional properties of two-pore-domain potassium channels. Am J Physiol Renal Physiol 279:F793–F801
46. Patel AJ, Honore E (2001) Molecular physiology of oxygen-sensitive potassium channels. Eur Respir J 18:221–227